Title:

Time-frequency domain analyses of the multi-channel electrocorticogram in the primary visual cortex of the hooded rat

Authors: Hirohito Sawahata[1], Haruo Toda[1], Takafumi Suzuki[2], Isao Hasegawa[1]

[1]Department of Physiology, Niigata University Graduate School of Medical and Dental Sciences
1-757 Asahimachi St, Chuo-ku, Niigata 951-8510, JAPAN
Phone: +81-25-227-2068
Fax: +81-25-227-0755

[2]Department of Mathematical and Information Physics, Faculty of Engineering, The University of Tokyo
7-3-1 Hongo, Bunkyo-ku, Tokyo 113-8654, JAPAN
Phone: +81-3-5841-6880
Fax: +81-3-5841-6882

Manuscript Type: Full original paper
Running title: Time-frequency analysis of ECoG inV1
Corresponding Author: Hirohito Sawahata
Corresponding Author's Institution: Niigata University

SUMMARY

The primary visual cortex (V1) of the rat consists of a monocular (contralateral-eye-dominant) region (V1M) and a binocular region (V1B) that receives anatomical and functional inputs converging from both eyes. However, V1B contains a heterogeneous mosaic of neurons stochastically discharging with various degrees of ocular dominance, and it has been difficult to estimate the size and behavior of the neuronal populations recruited by stimulation to individual eyes. To functionally characterize the V1B, we explore the similarities and differences of activation patterns between the contralateral and ipsilateral visual stimulation conditions in V1. Using a high density electrode array, 32-channel electrocorticogram (ECoG) was recorded from the whole surface of V1 of anesthetized Long-Evans rats. Despite a similarity of the spatial activation patterns in the early phase, contralateral eye stimulation evoked consistently stronger responses and higher signal coherency between the most responsive site and adjacent sites than ipsilateral stimulation. Time-frequency analyses confirmed that contralateral activations were more widely distributed from V1B to V1M in low frequency powers (2-30 Hz). On the other hand, high frequency powers (30-100 Hz) were localized in V1B. These findings revealed time-frequency domain properties of V1B. We speculate that the sustained high frequency activity reflected visual information flow from V1B to higher cortical centers.

Key words: MEMS electrode; spectral analysis; ocular dominance

INTRODUCTION

Electrocorcicogram (ECoG) is a method to electrically record neuronal activities at the surface of the cerebral cortex. ECoG is less invasive than intracortical microelectrode methods and has more time-accuracy than functional magnetic resonance imaging (fMRI) or optical imaging techniques. Recently, high-density ECoG recordings with "micro-ECoG arrays" were reported by several laboratories [1-3], yielding higher spatial resolutions than conventional silver ball electrodes or clinically used ECoG arrays which had large (1 mm in diameter or larger) electrode contacts with 10 mm interelectrode spacing. In a previous study [4], we newly developed an ultra-thin and flexible micro-ECoG array (ECoG-mesh). At a cost of fragility, the ultra-thin flexible ECoG-mesh was laid on cortical surface stably. Consequently, multi-channel ECoG signal was stably recorded in both acute and chronic experiments. Although ECoG cannot directly examine the vertical organization of the cortex across layers, the ECoG-mesh has fenestrae between electrodes, which allow penetration of the depth recording electrodes. We found that significantly correlated signals between ECoG-mesh and intracortical microelectrodes (unit activities and local field potentials) in primary visual cortex (V1) of Long-Evans (hooded) rats. The fenestrae could also be used for cortical stimulation, which was not capable by the ECoG-mesh itself because, at the current moment, the ultra-thin gold electrode did not endure large electrical currents. In addition, we developed minimally-invasive neurosurgical protocols to place a modified ECoG-mesh within cerebral sulci of the macaque monkey [5].

The present study aims to test the feasibility of the high-density ECoG-mesh in time-frequency domain analyses by focusing on a functional unit termed "binocular region" in V1 of Long-Evans rats. Unlike V1 of the primates and cats, the rat V1 is separated into two regions according to the ocular dominance; the monocular region (V1M) which receives visual inputs only from the contralateral eye and the binocular region (V1B) which receives projections from both eyes, analogous to primate V1. Despite anatomical and functional inputs converging

from both eyes [6-8], the rat V1B contains a heterogeneous mosaic of neurons stochastically discharging with various degrees of ocular dominance [9, 10]. The neuron-to-neuron diversity and trial-to-trial variability [11], together with complexity of distributed cortical interactions [12], make it difficult to estimate the size and behavior of neuronal populations recruited by stimulation to individual eyes. To resolve this issue we used the multi-channel ECoG method that is suitable for recording the neuronal population activity. We examined the similarities and differences between the ECoG responses to contralateral and ipsilateral visual stimulations. For this purpose, visually evoked ECoG signals were analyzed in domain of time, frequency and spatial distributions.

MATERIALS and METHODS

ECoG electrode array

The ECoG mesh was designed to cover 6 mm x 6 mm cortical areas with inter-electrode distance of 1-mm (Figure 1A), much closer than conventional clinical-use ECoG probe. The thickness of the ECoG mesh was 20 μm, much thinner than clinical-use ECoG probe. Our ECoG probe had a mesh structure with large fenestrae (800 μm x 800 μm), or holes, open between electrodes. Out of the 36 electrode on an ECoG-mesh, 32 were for recording (filled squares in Figure 1B), 4 were for reference/ground (open squares in Figure 1B).

Animal preparation

Data were obtained from six hemispheres in three adult rats (Long-Evans, 300-400 g). The rats were anesthetized by intraperitoneal injection of urethane (0.5 ml of 30% solution/100g body weight). Part of the cranium was removed to place the flexible ECoG mesh on the dura mater. The craniotomized areas were 2-9 mm caudal and 1-7 mm lateral to bregma. These areas corresponded to V1 and adjacent the secondary visual cortex (V2), but the caudal tip of V1 was not included (Figure 1B). The rostral end of ECoG mesh was located on the parietal association cortices. All procedures were approved by the Niigata University Animal Experiment Committee, and conformed to guidelines of the animal welfare laws in Japan and NIH Guide for the Care and Use of Laboratory Animals.

Visual stimulation

As visual stimuli, moving sinusoidal gratings were presented on a cathode ray tube monitor (EIZO T561, Nanao Corp., Ishikawa, Japan) placed 28.6 cm in front of the animal. Stimulus duration was 500 ms and the inter-trial-interval duration was pseudo-randomly chosen between 1.5-2.0 sec. Stimuli were generated using the ViSaGe (Cambridge Research Systems)

controlled by software written in FreePascal/Lazarus and run on Windows XP. Spatial- (0.04-0.15 cycle/deg) and temporal (3-7 Hz) grating frequencies were used according to Girman[11]. In the contralateral (Contra) and ipsilateral (Ipsi) stimulation conditions, the eye ipsilateral or contralateral to the recording side was covered with an eye patch, respectively. Stimulation was performed in separate blocks, consisting of 40-200 trials each. In certain trials, both eyes were covered with eye patches to ensure that the visual stimuli were effectively blocked.

Recordings and data acquisition

The recording sessions took 3-6 hours. Total experimental time was 5-8 hours/hemisphere. Signals from the ECoG mesh were amplified using a 32-channel amplifier (Plexon Inc., Texas, U.S.A.) with 300 Hz and 0.7 Hz cut-off frequencies. The signals were acquired and stored onto a hard disk, using custom-made data acquisition software (NS Computer Systems Inc., Nagaoka, Japan) running on the LabVIEW system (National Instruments Inc., U.S.A.) for Windows XP with DAC boards (National Instruments Inc., U.S.A.). Sampling frequency was 1 kHz.

Spatial similarity between the Contra and Ipsi stimulation condition

A spatial pattern vector for each of the Contra and Ipsi stimulation conditions was defined from an across-trial average of the ECoG signals. Then, 'spatial similarity' was calculated utilizing Pearson's correlation coefficient between the spatial pattern vectors in Contra and Ipsi stimulation conditions.

Local coherency

The cross-correlation function between signals from the most responsive electrode and

surrounding 4 electrodes during each time window (-400 – -200, -200 – 0, 0 – 200, 200 – 400 and 400 – 600 ms) was calculated. The maximum value of the cross-correlation function was defined as the local coherency. Its range is from 0 to 1. The local coherency was 1 if signals from 5 electrodes was identical.

Time-frequency domain analysis

Time-frequency plots (spectrogram) of ECoG signals were calculated using the short-time Fourier transformation method in a trial-to-trial manner with a sliding time window (hanning window function, width of 500 ms and 10 ms step). The plots were averaged over all trials, and then the mean power spectrum during pre-stimulus period (-1000 to -500 ms from stimulus onset) was subtracted to normalize the logarithm of power. The time and frequency resolutions were 10 ms and 2 Hz, respectively. The spectrogram analysis was done with MATLAB (Mathworks; Natick, MA, U.S.A.). The remaining of off-line data analysis were performed with custom-made software written in FreePascal/Lazarus and a free statistical software GNU R (http://www.r-project.org/) on Macintosh computers.

Analysis of visually evoked potentials

In some analyses, visually evoked potentials (VEPs) were normalized using following procedures. For each channel and trial, the resting activity was estimated by calculating mean and standard deviation (SD) for each pre-stimulus period (0-500 ms prior to stimulation onset). The pre-stimulus mean voltage was subtracted from observed voltages of the corresponding channel and trial, and subsequently divided by the pre-stimulus SD to acquire normalized voltages. Data were divided into 10-ms bins to compare normalized voltages and then voltages were averaged over the whole channels and entire trials within each bin. Responding electrodes at a sampling time were defined as electrodes with normalized VEP voltages > 3. The numbers

of responding electrodes were averaged in the same way as the normalized amplitudes.

Statistics

Results are expressed as means ± standard error of mean (S.E.M) unless otherwise mentioned. Differences were tested using Student's *t*-test. In the most pair-wise comparisons, results from the same hemispheres were paired. However, electrode coordinates with the same order in both stimulations were paired to test the lateral shift of VEP peak positions. All statistical calculations were performed using a free statistical software GNU R.

RESULTS

In the Contra stimulation trials, VEPs were observed in the whole field of V1 (Figure 2A). In contrast, VEPs in the Ipsi stimulation trials were obviously smaller and more spatially limited (Figure 2B). The differences in amplitudes of VEPs between conditions remained significant even after trial-to-trial normalization (1.17 ± 0.18 and 0.21 ± 0.10, respectively, $P < 0.01$, Figure 2C). The number of responding electrodes after trial-wise normalization was also significantly different between conditions ($P < 0.005$, Figure 2D).

The initially responding sites were similar in both Contra and Ipsi conditions. In both conditions, initial visual responses were found during 50-to-99-ms period following the stimulus onset in coordinates IV to V and c to d (Figure 3A). The similarity between the spatial patterns of the Contra and Ipsi trials in each sampling time was estimated by the correlation coefficient r (Figure 3B). In the prestimulus period, correlation coefficients were not significantly different from zero, but 50 to 100 ms after the stimulation onset, correlation coefficients rose above the $r = 0.44$ ($p < 0.01$, $df = 30$) line (dashed line in Figure 3B) in all six hemispheres, then correlation coefficients fell to zero again. This result means that the similar region was activated under both Contra and Ipsi stimulation conditions in the early phase of visual activity.

We further compared the local coherency surrounding the most responsive electrode between conditions. In the Contra condition, correlation increased in many electrodes following stimulus onset (Figure 4). In contrast, these increases were not detected in the Ipsi trials. Statistically significant differences were found between both stimulation conditions in the 0-200-ms and 100-300-ms time windows. These results indicate that contralateral stimulation induced a coherent activity in a local cortical area, but ipsilateral stimulation did not.

Time-frequency analysis (Figure 5A) of visually-induced ECoG signals not only confirmed Contra dominancy of the signal power and distribution, but also revealed time- and frequency- specificity of the signals. At least two signal components were distinguished: a tonic

component mainly in higher (gamma band) frequencies (30-100 Hz), and a phasic component primarily observed in lower frequencies (2-28 Hz). The phasic lower-frequency peak was distributed across many electrodes specifically in the Contra condition, whereas the tonic gamma-band peak was localized to a few electrodes in both conditions (Figure 5B).

Significant differences in the maximum power between the Contra and Ipsi conditions were found in both low- (3.72 ± 0.43 and 1.32 ± 0.26, respectively) and high frequency bands (1.75 ± 0.14 and 1.05 ± 0.18, respectively) in all six hemispheres (Figures 6A and B). In lower and higher frequencies, the number of channels that significantly increased power in Contra condition was more than in Ipsi condition (Figure 6C).

DISCUSSION

In the present paper, we used micro ECoG to functionally characterize activation patterns by Ipsi and Contra eye stimulation in the rat V1. Amplitudes, spectral powers, and synchronization of the Ipsi-induced ECoG signals were consistently smaller than Contra-induced signals, even in the binocular visual cortex. The assignment of the binocular and monocular V1 regions was confirmed with intracortical unit recording from a tungsten microelectrode [6-8].

In both Contra and Ipsi conditions, initially responding sites were localized in the same region in V1, corresponding to the representation of nasal visual field where the visual stimuli were presented. Activity spreads from here to many directions, typically toward mediocaudally in the Contra condition, but less extensively in the Ipsi condition (Figure 3A). The stereotaxic coordinates of Ipsi-activated region were in agreement with those of V1B [9, 10, 13-15]. Smaller VEP in the Ipsi condition might be attributable not only to smaller number of recruited cells, but also to lack of stimulation-induced synchronization in Ipsi-induced VEPs (Figure 4), presumably reflecting sparseness of ipsilateral thalamocortical projections [16].

In the Contra condition, VEPs were primarily located in V1 (Figure 2). But the signals occasionally spread out rostrally. Although shunt currents might account for such wide spreads, two lines of evidence could not solely be explained by this possibility. First, we observed significant regional differences between the Contra and Ipsi conditions in spatial extents of normalized activation (Figure 6D) and stimulation-induced synchronization (Figure 4). Second, correlations were disproportionately smaller at rostralmost electrodes than other electrodes (unpublished data). Taken together, the distributed VEP patterns would reflect cortical signal processing, rather than mere shunt currents. This finding was consistent with other studies indicating that the supra- and sub-threshold cortical signals traverse across classically defined primary sensory areas such as the primary visual, auditory and somatosensory areas in the rodents [17, 18].

The gamma frequency was thought to be involved in bottom-up synchronization from the visual- to higher-cortices in humans [19, 20] and monkeys [21-25]. The peaks localized in a limited region, rostral to the center of low frequency peaks in the Contra condition, presumably corresponding to the boundary between V1B and the anterolateral (AL) subarea of V2. AL is one of the motional vision-related subareas in rat, possible homologue of posteromedial lateral suprasylvian area (PMLS) of cat or middle temporal (MT) of primates [25-29]. Therefore, it was likely that sustained high frequency activity reflected visual information flow from V1 to higher centers.

Reference

1. Hollenberg BA, Richards CD, Richards R, Bahr DF, Rector DM: A MEMS fabricated flexible electrode array for recording surface field potentials. J Neurosci Methods. 153: 147-153, 2006.

2. Rubehn B, Bosman C, Oostenveld R, Fries P, Stieglitz T: A MEMS-based flexible multichannel ECoG-electrode array. J Neural Eng. 6: 036003, 2009.

3. Kim DH, Viventi J, Amsden JJ, Xiao J, Vigeland L, Kim YS, Blanco JA, Panilaitis B, Frechette ES, Contreras D, Kaplan DL, Omenetto FG, Huang Y, Hwang KC, Zakin MR, Litt B, Rogers JA: Dissolvable films of silk fibroin for ultrathin conformal bio-integrated electronics. Nat Mater. 9: 511–517, 2010.

4. Toda H, Suzuki T, Sawahata H, Majima K, Kamitani Y, Hasegawa I: Simultaneous recording of ECoG and intracortical neuronal activity using a flexible multichannel electrode-mesh in visual cortex. Neuroimage. 54: 203-12, 2010.

5. Matsuo T, Kawasaki K, Osada T, Sawahata H, Suzuki T, Shibata M, Miyakawa N, Nakahara K, Iijima A, Sato N, Kawai K, Saito N, Hasegawa I: Intrasulcal electrocorticography in macaque monkeys with minimally invasive neurosurgical protocols. Front Syst Neurosci. 2011.

6. Coway A, Perry VH: The projection of the temporal retina in rats, studied by retrograde transport of horseradhish peroxidase. Exp. Brain Res. 35: 457-464, 1979.

7. Drager UC, Olson J: Origins of crossed and uncrossed retinal projections in pigmented and albino mice. J. Comp. Neurol. 191: 383-412, 1980.

8. Ohashi K, Tanaka S: Visualization of neural activity in the rat visual cortex with intrinsic optical imaging. International Congress Series. 1269 85-88, 2004.

9. Diao YC, Wang YK, Pu ML: Binocular Responses of Cortical Cells and the Callosal Projection in the Albino Rat. Exp. Brain Res. 49: 410-418, 1983.

10. Thurlow GA, Cooper RM: Metabolic Activity in Striate and Extrastriate Cortex in the Hooded Rat: Contralateral and IpsiLateral Eye Input. J. Comp. Neurol. 274: 595-607, 1988.

11. Cohen MR, Newsome WT: Estimates of the contribution of single neurons to perception depend on timescale and noise correlation. J. Neurosci. 29: 6635-6648, 2009.

12. Dahl CD, Logothetis NK, Kayser C: Spatial organization of multisensory responses in temporal association cortex. J. Neurosci. 29: 11924-11932, 2009.

13. Espinoza SG, Thomas HC: Retinotopic organization of striate and extrastriate visual cortex in the hooded rat. Brain Res. 272: 137-144, 1983.

14. Gias C, Hewson-Stoate N, Jones M, Johnston D, Mayhew JE, Coffey PJ: Retinotopy within rat primary visual cortex using optical imaging. NeuroImage. 24: 200-206, 2005.

15. Zilles K, Wree A, Schleicher A, Divac I: The Monocular and Binocular Subfields of the Rat's Primary Visual Cortex: A Quantitative Morphological Approach. J. Comp. Neurol. 226: 391-402, 1984.

16. Reese BE, Cowey A: Large retinal ganglion cells in the rat: their distribution and laterality of projection. Exp. Brain Res. 61: 375-385, 1986.

17. Frostig RD, Xiong Y, Chen-Bee CH, Kvasˇnˇák E, Stehberg J: Large-Scale Organization of Rat Sensorimotor Cortex Based on a Motif of Large Activation Spreads. J. Neurosci. 28: 13274-13284, 2008.

18. Kamatani D, Hishida R, Kudoh M, Shibuki K: Experience-dependent formation of activity propagation patterns at the somatosensory S1 and S2 boundary in rat cortical slices. NeuroImage. 35: 47-57, 2007.

19. Melloni L, Molina C, Pena M, Torres D, Singer W, Rodriguez E: Synchronization of Neural Activity across Cortical Areas Correlates with Conscious Perception. J. Neurosci. 27: 2858-2865, 2007.

20. Werkle-Bergner M, S ller V, Li S, Lindenberger U: EEG gamma band synchronization in visual coding from childhood to old age: Evidence from evoked power and inter-trial phase locking. Clinical Neurophysiol. 120: 1291-1302, 2009.

21. Buschman TJ, Miller EK: Top-down versus bottom-up control of attention in the prefrontal and posterior parietal cortices. Science. 315: 1860-1862, 2007.

22. Fries P: Neuronal gamma-band synchronization as a fundamental process in cortical computation. Annu. Rev. Neurosci. 32: 209-224, 2009.

23. Hasegawa I, Fukushima T, Ihara T, Miyashita Y: Callosal window between prefrontal cortices: cognitive interaction to retrieve long-term memory. Science. 281: 814-818, 1998.

24. Tallon-Baudry C: The roles of gamma-band oscillatory synchrony in human visual cognition. Front. Biosci. 14: 321-332, 2009.

25. Coogan TA, Burkhalter A: Hierarchical Organization of Areas in Rat Visual Cortex. J. Neurosci. 3: 3749-3772, 1993.

26. Harvey AR, Worthington DR: The Projection From Different Visual Cortical Areas to the Rat Superior Colliculus. J. Comp. Neurol. 298: 281-292, 1990.

27. Montero VM, Jian S: Induction of c-fos protein by patterned visual stimulation in central visual pathways of the rat. Brain Res. 690: 189-199, 1995.

28. Rumberger A, Tyler ACJ, Lund JS: Intra- and inter-areal connections between the primary visual cortex V1 and the area immediately surrounding V1 in the rat. Neurosci. 102: 35-52, 2001.

29. Toda H, Tanimoto N, Takagi M, Abe H, Bando T: Visual cortical contribution to open-loop and feed-back control of convergence eye movements in the cat. Neurosci. Res. 54: 302-312, 2006.

Figure legends

Figure 1

A: Structure of an electrocorticogram electrode mesh (ECoG-mesh). 36 electrodes (50 x 50 μm) were coated with platinum black to decrease the impedance (1 k- 20 kΩ in saline (at 1 kHz)). Electrodes were arranged in a 6 x 6 array with 1-mm interelectrode distance, wired within a flexible Parylene-C (poly(chloro-para-xylylene)) substrate of 20-μm thick, and connected to a terminal. Between electrodes, holes (800 x 800 μm) were open through the substrate.

B: Approximate area covered by ECoG mesh. Thirty two recording electrodes (filled squares) and 4 reference/ground electrodes (open squares) were placed on the dura mater. The positional variations of ECoG mesh across all experiments were < 1 mm in rostrocaudal and mediolateral directions. The cortical map was reconstructed from *The Rat Brain* [Paxinos and Watson, 2007]. V1, primary visual cortex; M, monocular area; B, binocular area; V2, secondary visual cortex; TeA, temporal association cortex; MPtA, medial parietal association cortex; LPtA, Lateral parietal association cortex; Pt, parietal cortex; Au, auditory cortex; S1, primary somatosensory cortex; S2, secondary somatosensory cortex; M1, primary motor cortex; M2, secondary motor cortex; RSD, retrosplenial dysgranular cortex.

Figure 2

A and B: Examples of averaged visually evoked potentials (VEPs) recorded from each electrode in the ECoG mesh from the right hemisphere of a rat. The traces are arranged with reference to spatial positions of the electrodes. The numbers of averaged trials were 80 in each of contralateral (Contra) and ipsilateral (Ipsi) conditions, respectively. In each trace, the vertical bar indicates the stimulus onset. Scale bar = 0.2 mV, 500 ms. A: anterior (rostral), L: lateral.

C: Normalized voltage 90-99 ms following stimulus onset. Each bar represents the mean of six

hemispheres. White bar: Contra, Gray bar: Ipsi. The different symbol indicates a different hemisphere.

D: Numbers of responding electrodes 100-109 ms after stimulus onset. Formats are the same as C.

Figure 3

A: An example of time course in the spatial VEP patterns in a hemisphere following stimulation onset in the Contra and Ipsi conditions. The axes are the same as Figure 1B. Each circle represents electrode position and the diameter represents the corresponding mean VEP voltage recorded with the electrode. The circle color (red or blue) indicates voltage polarity (red : positive, blue : negative). Circles below the labels 'Contra' and 'Ipsi' are scales (0.1 mV).

B: The averaged spatial similarities between the Contra and Ipsi trials as a function of time. The mean $r \pm$ standard errors of six hemispheres are displayed in thick and thin lines. These traces were smoothed using a 2nd- and 3rd-order polynomial convolution method [29]. The vertical line indicates the stimulation onset. The horizontal, dashed lines indicate $r = \pm 0.44$ ($p < 0.01$).

Figure 4

The maximum value of the cross-correlation function between signals from the most responsive electrode and surrounding 4 electrodes during each time window. The ordinates indicates maximum value of cross-correlation function. Abscissa indicates time ranges for calculation of the cross-correlation. Open circle: the Contra condition, closed circle: the Ipsi condition.

Figure 5

A: Representative spectrograms of the VEPs in Contra and Ipsi conditions. In each panel, the ordinate and abscissa indicate the frequency and time after stimulus onset, respectively. Data and

plot arrangement were the same as in Figure 2.

B. The maximum low frequency (2-28 Hz) and high frequency (30-100 Hz) powers observed at each electrode in a 1-s period immediately following stimulus onset in each of the stimulation conditions in A.

Figure 6

A and B: Maximum low frequency (A) and high frequency (B) powers in a 1-s period immediately following the stimulus onset averaged over electrodes.

C: The number of channels that significantly increased powers in low and high frequency bands. Formats are the same as Figure 2C.

Figure 1

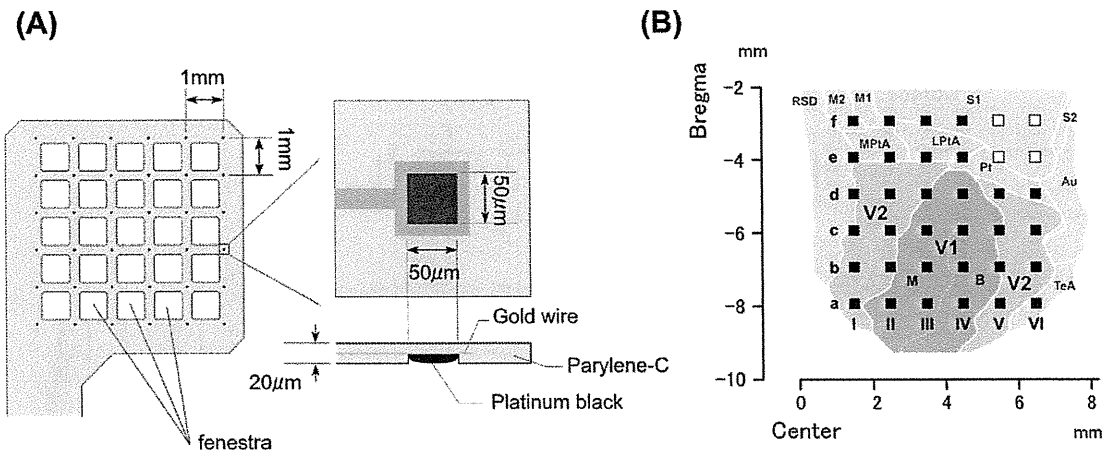
(A)
1mm
1mm
50μm
50μm
Gold wire
Parylene-C
20μm
Platinum black
fenestra
(B)
mm
Bregma
−2
−4
−6
−8
−10
RSD
M2
M1
S1
S2
f
e
d
c
b
a
MPtA
LPtA
Pt
Au
V2
V1
M
B
V2
TeA
I
II
III
IV
V
VI
0
2
4
6
8
Center
mm

Figure 2

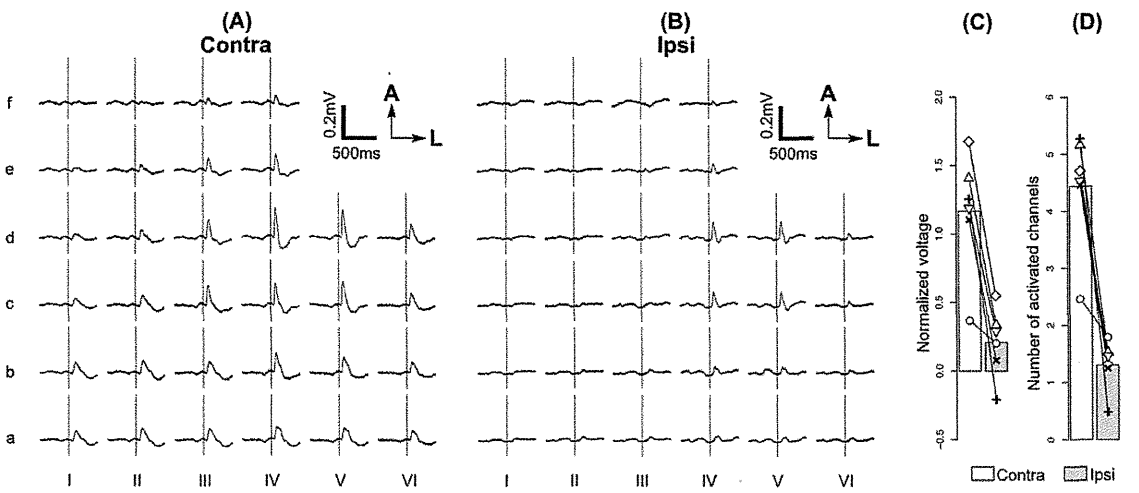
(A)
Contra
(B)
Ipsi
(C)
(D)
f
e
d
c
b
a
0.2mV
500ms
A
L
I
II
III
IV
V
VI
Normalized voltage
Number of activated channels
Contra
Ipsi

Figure 3

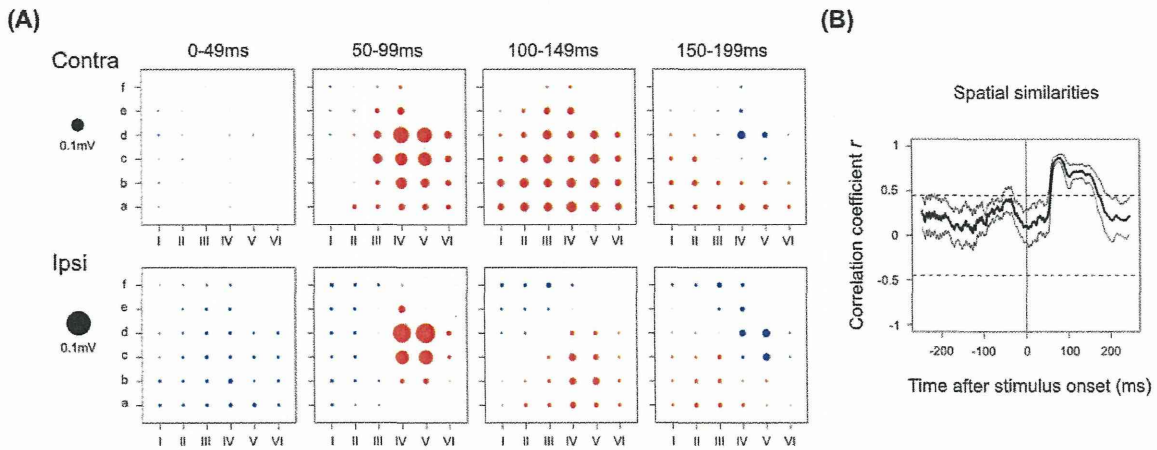
(A)
Contra
0-49ms
50-99ms
100-149ms
150-199ms
0.1mV
Ipsi
0.1mV
(B)
Spatial similarities
Correlation coefficient r
Time after stimulus onset (ms)